Investigation of Proton Dynamics within the Hydrogen-Bond Network of the Layer Silicate Na−RUB-18

Markus Borowski, Ingo Wolf, and Hermann Gies*

Institut für Geologie, Mineralogie und Geophysik, Ruhr-Universität Bochum, D-44780 Bochum, Germany

Received December 19, 2000. Revised Manuscript Received July 27, 2001

Solid-state ^{1}H and ^{29}Si MAS NMR spectroscopies were applied to the hydrous layer silicate Na−RUB-18 to investigate the hydrogen-bond networks formed within the crystals as a function of temperature. Two different proton environments can be differentiated. At temperatures below 230 K, the weak hydrogen bonds formed by the intercalate water and the strong hydrogen bonds formed by the silanol groups do not interact. At temperatures up to 360 K, an increasing number of hydrogen bonds localized at silanol groups breaks up. At this temperature, 1D infinite hydrogen-bond networks are formed in the material, resulting in proton conductivity. Molecular dynamics (MD) simulations yielded increasing vibrations of these hydrogen bonds as an explanation for the breaking. From ^{1}H MAS NMR experiments with modified samples, it becomes obvious that only one-half of all water molecules participate in the network. Further, it is shown that a mimimum coherence of the 1D network is necessary to stabilize the high-temperature state.

Introduction

MAS NMR spectroscopy is a powerful tool for investigating dynamic processes in crystalline and amorphous solids. By the nature of this technique, the time scale for dynamic processes to be studied is on the order of microseconds up to seconds, and therefore, it is complementary to, for example, neutron and X-ray diffraction studies. A benefit of NMR techniques is the possibility of studying nuclei in different chemical environments within one sample, as they can be discerned from one another because of their individual resonance frequencies. In the present investigation, this property was helpful in developing a model of the proton dynamics in the hydrous layer silicate Na−RUB-18.[1,2]

Layer silicates such as Na−RUB-18 are a group of materials[3−5] that recently has been of considerable interest for industrial applications in catalysis and ion exchange. They attract particular attention because of their high ion exchange capacity[6,7] and their potential to modify geometrically and chemically the interlayer space through pillaring with various organic and inorganic building blocks.[8]

For basic scientific research, they hold the interesting feature of an extended internal silanol-terminated surface that is in close interaction with the intercalated water molecules and the charge-compensating cations of the interlayer space. Because these materials are crystalline, it is possible to study their structural properties with standard diffraction analysis and, in addition, the dynamics and reactions at the internal silicate/water interfaces using NMR spectroscopy. Results obtained from these model systems are valuable in understanding and describing fundamental processes at external surfaces, e.g., the mineral/water interface, which are important in various fields such as sorption, ion exchange, catalysis, rheology, or thermodynamics.

Unfortunately, the crystallinity of most of the layer silicates is poor, precluding a detailed study of their crystal structures. Na−RUB-18[2] ($Na_8[Si_{32}O_{64}(OH)_8]\cdot 32H_2O$) stands out in this respect: It has a perfect stacking order of the silicate layers and the charge-compensating interlayer hydrated cations. The structure was solved using X-ray powder-diffraction data with direct methods and refined including the hydrate/cation interlayer using Rietveld analysis.[2] Because of their low scattering power, the hydrogen atoms were not resolved. Figure 1 shows a simplified representation of the crystal structure, where the hydrogen atoms and the bridging oxygens of the silicate layers are omitted. Recently, neutron diffraction experiments were performed, providing a detailed picture of the bonding of the silanol and water protons.[9]

Na−RUB-18 crystallizes in the space group $I4_1/amd$. In the silicate layers, the ratio of Q^3 silicons (bound to three $[SiO_4]$ tetrahedra and one OH group) to Q^4 silicons (bound only to $[SiO_4]$) is 1:1. Within the structure, every other Q^3 silanol group is deprotonated. As a conse-

(1) Iler, R. *J. Colloid Sci.* **1964**, *19*, 648.
(2) Vortmann, S.; Rius, J.; Siegmann, S.; Gies, H. *J. Phys. Chem. B* **1997**, *101*, 1292.
(3) Eugster, H. P. *Science* **1967**, *157*, 1177.
(4) Benke, K. H.; Lagaly, G. *Am. Mineral.* **1983**, *68*, 818.
(5) Schwieger, W.; Bergk, K. H. *Z. Chemie* **1985**, *6*, 228.
(6) Kosuge, K.; Singh, P. S. *Chem. Mater.* **2000**, *12*, 421.
(7) Rieck, H. P. *Nachr. Chem. Tech. Lab.* **1996**, *44*, 699.
(8) Bergk, K. H.; Schwieger, W.; Porsch, M. *Chem. Technol.* **1987**, *11*, 459.
(9) Borowski, M.; Asmussen, B.; Gies, H. *Z. Kristallogr. Suppl.* **2001**, *18*, 94.

10.1021/cm0012522 CCC: $22.00
Published on Web 12/18/2001

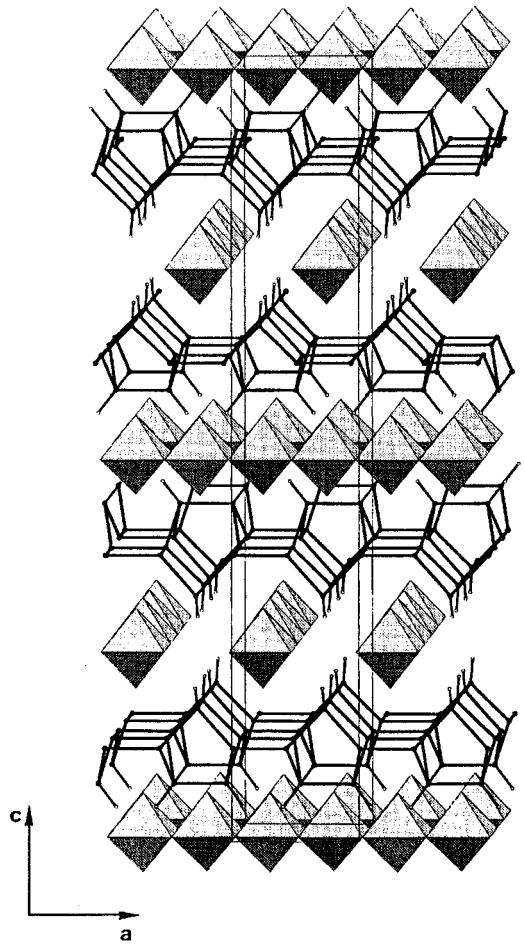

Figure 1. Perspective view of the crystal structure of Na−RUB-18 as determined by X-ray diffraction. The silicate layer is represented as skeleton model showing only the silicon atoms and the oxygens belonging to the silanol groups. The bonding oxygen atoms, located in the middle of the Si···Si bonds, and the hydrogen atoms are not shown for clarity. The sodium cations are coordinated octahedrally by water molecules in the interlayer space. These $[Na(H_2O)_6]^+$ octahedra form one-dimensional edge-linked chains.

quence, a hydrogen bond is formed between the neighboring Si−OH and Si−O$^-$ groups that is very strong as the O−O distance is only about 2.3 Å. The strong deshielding of the proton in this hydrogen bond results in a downfield chemical shift of ∼16.3 ppm relative to tetramethylsilane (TMS) in the ^{1}H MAS NMR spectrum (Figure 2, top). On the time scale of the NMR experiment, the proton in the hydrogen bridge is shared between both oxygen atoms, yielding in the ^{29}Si spectrum only one Q^3 signal at −99 ppm relative to TMS and not two, corresponding to the NMR-discernible Si−OH and Si−O$^-$ situation (Figure 2, bottom). Also, recently published ^{2}H and ^{17}O NMR studies of Na−RUB-18 found the silanol proton to be shared between the oxygen atoms.[10]

The negative charge of the silicate layer is compensated by sodium cations that are octahedrally coordinated by water molecules in the interlayer space (Figure 1). The $Na(H_2O)_6$ octahedra share edges, building 1D chains parallel to [100] and [010]. Only one signal at a

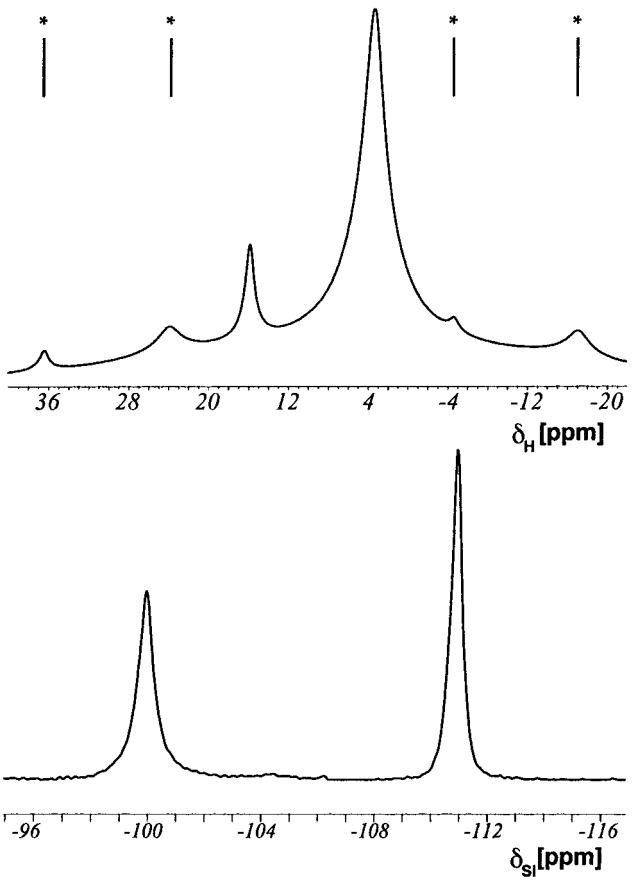

Figure 2. (Top) ^{1}H MAS NMR spectrum of Na−RUB-18 shows two proton positions (∼3.7 and ∼16.3 ppm) and corresponding spinning sidebands (*). The intensity ratio of the two signals is ∼8:1. (Bottom) ^{29}Si MAS NMR spectrum of Na−RUB-18 consists of two signals due to the Q^3 (approximately −100 ppm) and Q^4 (approximately −111 ppm) silicon positions. The ratio of the signals is ∼1:1.

chemical shift of ∼3.7 ppm is observed in the ^{1}H MAS NMR spectrum for the protons belonging to the hydrate water molecules, which is well-separated from the signal of the silanol proton. 2D NOESY experiments revealed a slow, temperature-dependent exchange between the two proton species.[12] The intensity ratio of the signals of silanol and water protons is 1:8[11] as expected from the chemical composition and the structure analysis[2] of Na−RUB-18.

In this study, we report on NMR experiments analyzing the temperature dependence of dynamic processes involving silanol and hydrate-water protons. These studies provide information on possible proton conductivity properties of Na−RUB-18 and insight into exchange processes that might occur similarly at external silicate/water interfaces.

In addition to spectroscopic experiments, force-field MD simulations were performed. In recent years, computational experiments have been developed as a powerful complementary tool accessible to materials sciences. Simulations are useful for investigating the structure of materials and simulating their dynamic behavior, even under conditions that are out of reach for experimental studies. Also, this tool is particularly

(10) Brenn, U.; Ernst, H.; Freude, D.; Herrmann, R.; Jähnig, R.; Karge, H. G.; Kärger, J.; König, T.; Mädler, B.; Pingel, U.-T.; Prochnow, D.; Schwieger, W. *Microporous Mesoporous Mater.* **2000**, *40*, 43.

(11) Almond, G. G.; Harris, R. K.; Franklin, K. R. *J. Mater. Chem.* **1997**, *7*, 681.

(12) Wolf, I.; Gies, H.; Fyfe, C. A. *J. Phys. Chem. B* **1999**, *103*, 5933.

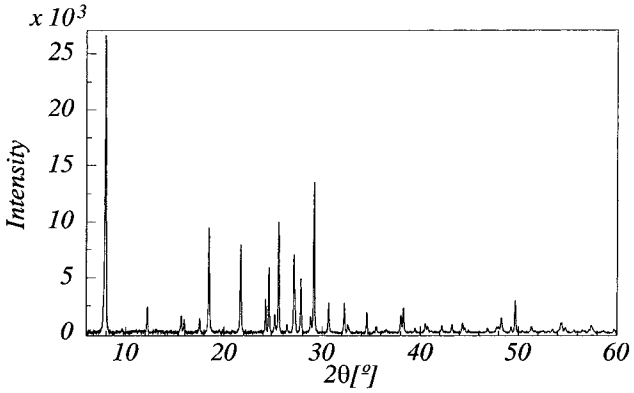

Figure 3. X-ray powder pattern of as-synthesized Na−RUB-18 (λ = 1.541 78 Å).

useful when either the experimental data are of insufficient quality or experiments are too time-consuming or expensive. The goal in our computational study is to extrapolate and rationalize experimental results with theoretical models of the proton dynamics, which otherwise would be difficult or even impossible to obtain.

Experimental Section

Materials. The Na−RUB-18 used for the present investigation was synthesized in the system SiO_2/NaOH/hexamethylenetetramine/triethanolamine/H_2O[13] in polyethylene bottles at 100 °C. In contrast to the synthesis reported in the literature,[2] CsOH was omitted. Highly crystalline Na−RUB-18 was obtained after four weeks, as verified by XRD measurements (Figure 3).

If not stated explicitly, all spectroscopic experiments were carried out on the as-synthesized material. In addition, certain modifications of Na−RUB-18 were performed, such as deuteration, partial dehydration, or doping with Cs^+ cations.

Na−RUB-18 was dehydrated to 50% by heating of the as-synthesized material for several weeks to 70 °C. The degree of dehydration was verified by Karl Fischer titration and thermogravimetry. The partially dehydrated sample was stored and transferred into NMR rotors under N_2 atmosphere.

A Cs-doped sample was prepared by replacing 4.3 % of the NaOH by CsOH in the materials synthesis. The Cs^+ ions were exchanged into Na−RUB-18 to replace Na^+ ions, as shown by AAS. In the sample used for the presented experiments, the degree of substitution was ∼5%.

NMR Spectroscopy. All NMR experiments were performed on a Bruker ASX-400 spectrometer. The ^{1}H MAS NMR experiments were run at a sample spinning rate of ∼10 kHz with a standard 4-mm probe. The recycle time was set to 1 s and, thus, was always longer than $10T_1$ of the protons in the sample.

The ^{1}H−^{29}Si CP MAS NMR experiments were run at a sample spinning rate of ∼4 kHz using a standard 7-mm probe. The Hartmann−Hahn condition for the 2D CP MAS measurements was set on the sample itself. The pulse lengths of the 90° pulse were 6 μs, the contact pulses were 0.5 ms.

Variable-temperature (VT) experiments were performed with the standard Bruker VT unit, with cooling below RT achieved by using N_2 gas. All chemical shifts were measured relative to tetramethylsilane (TMS) as the external standard. The signals were fitted with the program WINFIT.

MD Simulations. The MD simulations were performed with the software package InsightII[14] of MSI using a modified CVFF force field. Modification of the force-field parameters was necessary because the implemented values were found to be insufficient to describe layer silicates. The modifications were developed and tested using structural and physical properties of pure Na−RUB-18 itself. Using the force-field parameters in a constant-pressure run carried out at 298 K, the simulated structure reproduced the bond lengths and angles determined by X-ray diffraction[2] to within 1.7%. The compressibility of Na−RUB-18 along the lattice axes as determined by diffraction studies at pressures up to 5 GPa is reproduced to within 25% for the *a* and *b* axes and without any deviation for the *c* axis. Therefore, the force-field parameters are expected to be well-suited for the simulation of the material's dynamics.

As mentioned above and validated by density functional theory (DFT) energy-minimization calculations,[15] the silanol proton is shared by both silanol oxygens. To account for this feature, the silanol proton was not bound to a specific oxygen in the force-field simulation process but rather was held centered between the two oxygens by soft restraints in the form of spring potentials. In contrast, extended simulation calculations with single-bonded hydrogens failed to describe the structural features.

For the simulation of the structure, the symmetry was set to *P*1 including all 216 atoms of the tetragonal unit cell. For the simulation of the extended crystal, periodic boundary conditions were used. The energy calculation of long-distance interactions was done using Ewald summation with an accuracy of 0.586×10^{-3} kJ mol^{-1}. As the temperature range of the VT NMR measurements had to be covered, simulations were carried out between 100 and 450 K in steps of 20 K at constant pressure, thus allowing for adjustment of the lattice parameters due to thermal expansion.

Each simulation run was divided into two steps. First, the system was equilibrated for 200 fs using 0.2-fs stepwidth. Thereafter, the production step ran for about 10 ps, using a step width of 0.1 fs to reliably describe the vibration of the O−H bonds.[16] In both steps, a Verlet velocity integrator[17] was used for propagation.

Because the simulation was intended to provide information about dynamic properties of the material, frames were stored every 5 fs during the production step so that the vibrations within the crystal could be analyzed with sufficient accuracy. From the stored frames, bond lengths and velocities were calculated.

Results and Discussion

^{1}H MAS NMR spectra of the as synthesized Na−RUB-18, measured in the temperature range between 198 and 398 K, are shown in Figure 4. Obviously, the integral intensity of the 16-ppm signal decreases with increasing temperature *T*. Below 248 K, additional line broadening is observed.

To calculate the signal intensities quantitatively, the ^{1}H spectra were fitted with three pseudo-Voigt profiles, one for the silanol signal I'_1, two for the water signal $I'_{2,3}$, and a baseline.

For a proper quantitative analysis of the measured intensities, it was necessary to take into account the general temperature dependence of the magnetization according to Curie's law ($I \propto T^{-1}$). The corrected total intensity $I_{sum} = \sum_{i=1}^{3} I'_1 T$ was found, as expected, to be constant in *T*. This shows that the overall intensity of the signal is constant. However, the contribution of the different signals I_1−I_3 to I_{sum} varies with *T*.

The measured intensity I_1 normalized to the intensity I_{1_0} measured at low temperatures is shown in Figure 5.

(13) Kleinsorge, M. Ph.D. Thesis, Ruhr-Universität Bochum, Bochum, Germany, 2000.
(14) *InsightII Molecular Modeling System, User's Guide*; BIOSYM/MSI: San Diego, CA, 1996.
(15) Borowski, M.; Gale, J. D.; Gies, H., to be published.
(16) Verlet, L. *Phys. Rev.* **1967**, *159*, 98.
(17) Jeffrey, G. A. *An Introduction to Hydrogen Bonding*; Oxford University Press: New York, 1997.

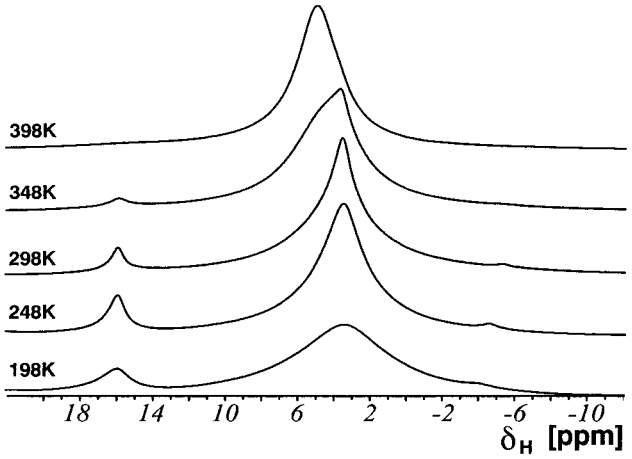

Figure 4. Temperature-resolved ^{1}H spectra of Na−RUB-18. The temperature dependence of the intensity and line width of the silanol proton signal (∼16 ppm) and the variation in the chemical shift of the water proton signal (∼4 ppm) are obvious.

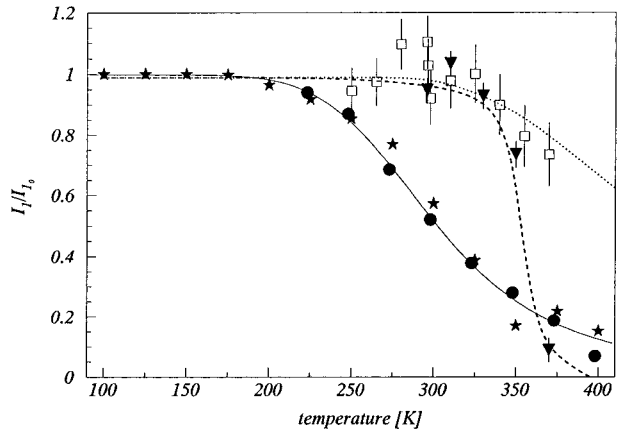

Figure 5. Temperature dependence of the relative intensity I_1/I_{1_0} of the silanol proton signal measured for different Na−RUB-18 samples with ^{1}H MAS NMR spectroscopy and calculated from MD simulations: ●, as-synthesized sample of Na−RUB-18; ★, results from MD simulations; solid line, curve fitted on the NMR data using eq 1 with $E_A \approx 20$ kJ mol^{-1}; ▼, partially dehydrated sample [the reduction of I_1/I_{1_0} takes place at increased temperatures (∼370 K), but this sample is qualitatively identical with the as-synthesized sample]; ■, Cs-ion doped sample (no overall breaking of the silanol hydrogen bonds is measured in the investigated temperature range). The dashed and dotted lines guide the eye on the temperature dependence of the ▼ and □ data, respectively.

The dependence can be described well by van't Hoof's law, assuming a transition of the silanol proton between two chemically inequivalent environments: one environment of the proton, responsible for the 16-ppm signal, that is mostly occupied at low temperatures and a second environment that becomes more and more occupied at elevated temperatures. The signal of the protons situated in the second environment appears as a low-field tail of the water resonance.

From the process explained above, it is easy to show that I_1 varies with T as

$$I_1 \propto \frac{1}{1 + k_A e^{-\Delta E/RT}} \qquad (1)$$

where ΔE is the energy difference between the two environments, R is the global gas constant, and k_A is the equilibrium constant. Later, it will be shown that the second environment is most likely entropically stabilized. A quantitative analysis of the data yields $\Delta E \approx 20$ kJ/mol and $k_A \approx 2600$. The temperature dependence of I_1 predicted by eq 1 is shown in Figure 5 as a solid line.

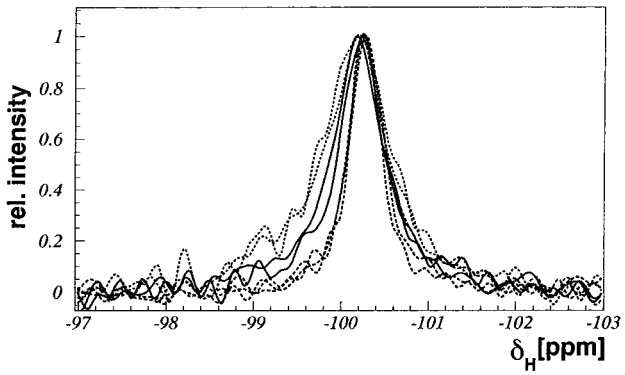

Figure 6. Q^3 signal of Na−RUB-18 measured in the temperature range between 230 and 380 K. The spectra measured at 230 and 250 K are shown as solid lines. The spectra measured at 270 and 298 K are shown as dotted lines. The spectra measured at 340, 360, and 380 K are shown as dashed lines. The change in silicon environment is obvious.

The different proton environments also result in different chemical environments for the corresponding silanol oxygens and, furthermore, for the Q^3 silicon atoms. Thus, at elevated temperatures, a second signal $Q^{3\prime}$ occurs in the ^{29}Si MAS NMR spectra. The difference in chemical shift between Q^3 and $Q^{3\prime}$ is very small compared to their line widths.

To eludicate the changes in chemical environment at the Q^3 site ^{1}H−^{29}Si CP MAS experiments were recorded in the temperature range between 230 and 380 K. Figure 6 shows an overlay of the Q^3 regions of the spectra measured at different temperatures. Three types of signal can be distinguished. At 230 and 250 K, a signal at −100.2 ppm is measured, corresponding to silicon in the proton low-temperature environment. The Q^3 signals measured at 270 and 298 K show considerable line broadening, corresponding to the transition between the low-temperature and high-temperature environments. At temperatures equal to or higher than 340 K, most of the protons are in the high-temperature environment. In the corresponding CP MAS spectra, again, a narrow but slightly high-field-shifted signal is observed. Thus, the ^{1}H−^{29}Si CP MAS spectra repoduce well the changes in proton environment already referred to in Figure 5.

^{1}H MAS and ^{1}H−^{29}Si CP MAS NMR experiments clearly demonstrate that the hydrogen atoms localized in the strong hydrogen bond at the silanol groups end up in a different environments at elevated temperatures.

To understand the mechanism of the process discussed above, force-field MD simulations were performed. Although the breaking of bonds, in principle, cannot be simulated with force-field simulations, the energies acting on bonds can be calculated. As was shown in the NMR experiments, the first proton environment is favored in comparison to the second one by an energy of ΔE. The first environment corresponds to

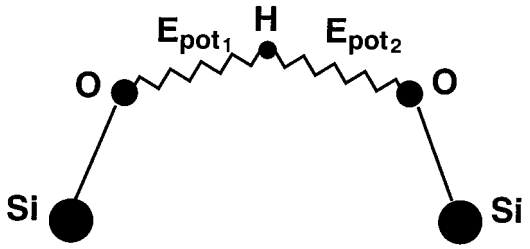

Figure 7. Sketch of a silanol hydrogen bridge in the Na−RUB-18 structure. Two potential forces symbolized by jagged line act on the hydrogen.

a situation in which the proton is shared by two silanol oxygens in a strong hydrogen bond. A schematic representation of the local situation is shown in Figure 7. In this environment, the proton can be regarded as being bound to both oxygens by equivalent spring potentials. At finite temperatures, the atoms move, causing potential energies that act on the bonds. As equivalent energies are stored in the two springs, the overall potential energy E_t of this local system can be calculated by $E_t = 2E_{pot}$, where E_{pot} is the potential energy stored in one

bond (see Figure 7). E_{pot} is determined by the actual bond length. In every frame n stored for analysis, E_{pot} was calculated for the silanol groups and also for the O−H bonds of the hydrate water molecules. Additionally, the kinetic energy E_{kin} stored in the stretching vibrations of the water molecules was calculated from the relative velocity $v_n = (d_n - d_{n-1})/\Delta t$ (Δt = 5 fs = time step between two stored frames) of the proton and the oxygen in a specified bond.

The details of the energy calculations are as follows:

$$E_{pot} = k_1(d-d_0)^2 \quad \text{for the silanol groups}$$

$$E_{pot} = k_2(1 - e^{k_3(d-d_0)^2}) \quad \text{(Morse potential) for the water molecules}$$

$$E_{kin} = \frac{1}{2}\mu v^2 \quad \text{kinetic energy of the OH stretching vibrations of the water molecules}$$

where k_i represents the force-field parameters; d and d_0 are the actual and reference bond lengths, respectively; and μ is the reduced mass [$= (1/m_1 + 1/m_2)^{-1}$] for a system consisting of two masses m_1 and m_2.

The energies were calculated for all silanol groups and eight water molecules in each frame stored. Average values of the energies ($\bar{E}_t$, $\bar{E}_{pot}$, $\bar{E}_{kin}$) for the water and the silanol groups were obtained by averaging the results first within each frame and then over all frames at a particular temperature.

In general, the absolute value of $\bar{E}_t$ is basically meaningless as the energy unit of force-field parameters k_i is arbitrary. For a realistic comparison between calculated and measured data, $\bar{E}_t$ had to be calibrated. The calibration was done using the energy stored in the stretching vibration of the O−H bonds of the water molecules. Each water molecule can be regarded as a free oscillator and, therefore, it fulfills $\bar{E}_{kin} = \bar{E}_{pot}$. In this equation, E_{kin} is independent of the force-field parameters, as it depends only on atomic masses and relative velocities. The energy conversion was done separately for each temperature. The temperature dependence of $\bar{E}_t$ shows the expected linear dependence.

It was assumed that, in the case of $E_t > \Delta E$ for a certain silanol group, the transition from the low-temperature to the high-temperature environment is induced. It is possible to calculate from a known $\bar{E}_t$ the fraction P of silanol groups for which $E_t < \Delta E$ at a certain temperature. The temperature dependence of P as calculated from the force field MD simulations is shown in Figure 5 using asterisks (*). The excellent agreement between the results of the simulation and the values obtained from the NMR experiments is obvious. This supports the hypothesis that the localized bonding positions become unfavorable at elevated temperatures as a result of thermal vibrations.

In the investigations presented above, the high-temperature environment of the protons was only regarded theoretically. To characterize the second environment and, thus, to explain how the state existing at elevated temperatures becomes stabilized, the influence of the intercalated hydrate water had to be included. For a description of the low-temperature environment, this was not necessary as, for a first approximation, it is decoupled from the rest of the intercalated water.

We propose that, in the high-temperature environment, the protons formerly shared by the silanol oxygens become completely delocalized in a 1D hydrogen-bond network consisting of the silanol groups and the equatorial water molecules of the sodium hydrate coordination octahedra (see Figure 8). This interpretation is consistent with pulsed field gradient NMR experiments that measured the temperature dependence of the diffusion coeffitients of the protons in the investigated range between room temperature and 330 K.[10] Our assumption also is supported by O···O distances of about 2.85 Å between the water and the silanol oxygens at these temperatures, which were extracted from neutron diffraction experiments.[9] In addition, the neutron diffraction studies show that the apical water molecules are isolated from the hydrogen-bond system. To validate the interpretation, two further NMR experiments were carried out. In the first experiment, it was shown that only the equatorial water molecules interact with the silanol groups in the high-temperature environment. The second experiment showed that the delocalization of the silanol protons in an extended hydrogen-bond network is needed to stabilize the high-temperature environment.

Temperature-dependent ^{1}H MAS NMR experiments were performed on a Na−RUB-18 sample that was dehydrated by 50%. The dehydration occurs in one step, leading to β-Na−RUB-18, leaving one-half of the hydration shell of the sodium cations. Upon dehydration, the c lattice parameter decreases by about 14%. These investigations led to the assumption that the apical water molecules of the Na hydration octahedra were removed selectively. Figure 9 displays the ^{1}H MAS NMR spectrum of β-Na−RUB-18, clearly showing the hydrogens involved in the strong hydrogen bridge at ∼14.8 ppm and the residual water protons. The measured intensity ratio is 1:4. As resulting from the compositions

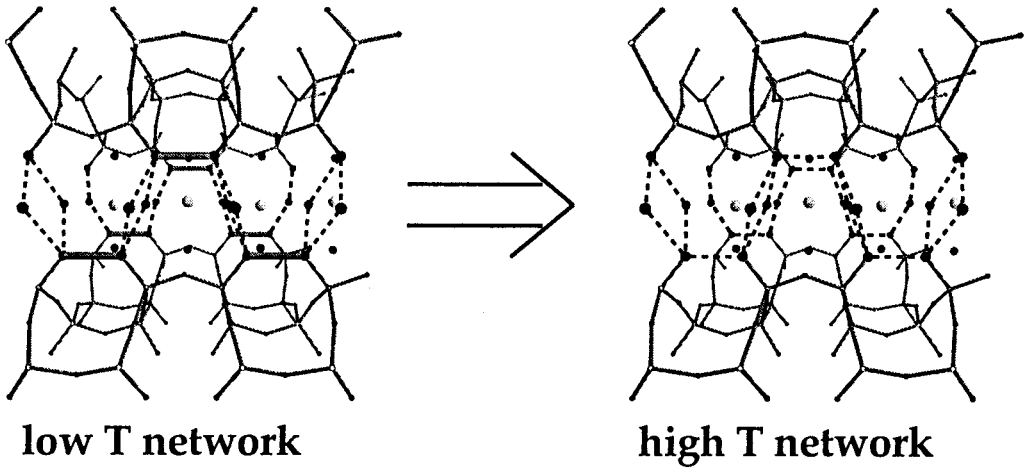

Figure 8. H-bond network at different temperatures. — represents a bond, ··· represents a hydrogen bond. At low temperatures, a localized silanol hydrogen bond and a four-membered ring of delocalized protons are observed. At higher temperatures, the silanol hydrogen bond breaks, giving rise to a 1D delocalized hydrogen-bond network.

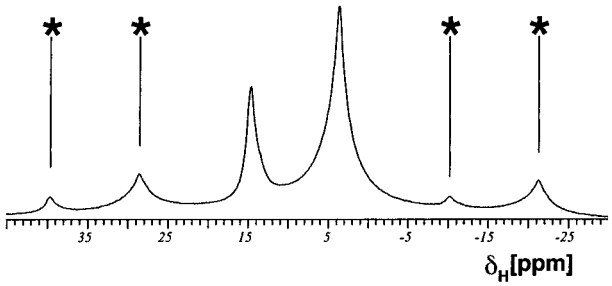

Figure 9. ^{1}H spectrum of partially dehydrated Na−RUB-18. In addition to the main signal, spinning sidebands are shown (*).

of β-Na−RUB-18 and Na−RUB-18, a comparison of the temperature dependence of their ^{1}H spectra provides information on the influence of the apical water molecules on the proton dynamics. The intensity of the silanol proton signal's measured temperature dependence is shown in Figure 5, demonstrating a temperature-dependent decrease of the I_1 signal. Compared to the as-synthesized Na−RUB-18, the decrease sets in at higher temperatures. This might be explained by distortions of the hydrogen-bond network due to minor structural changes that occur during the dehydration. Obviously, however, apical water molecules are not necessary for the formation of the high-temperature environment of the protons, confirming that only the equatorial water molecules are involved in the process.

In a second experiment, a sample was used in which Cs^+ replaced 4.3% of the Na^+ ions. Cs^+ ions have 1.7 times the size of the Na^+ ions, and thus, they most likely shift their coordinating water molecules markedly from the positions found in the original Na−RUB-18. In this case, the extended hydrogen-bond network is interrupted at positions in the crystal where Cs^+ resides. The experimental results of temperature-dependent ^{1}H MAS NMR studies are shown in Figure 5. Obviously, the creation of the high-temperature environment is supressed in this sample. According to our assumption, this can be explained by the fact that the substantially larger Cs^+ ions interrupt the extended hydrogen-bond network and, thus, limit the size of the 1D H-bond network to the distance between defect centers. The restriction of the available space reduces the entropy of the high-temperature environment and makes it less favorable. From our data, it is likely that a minimum network size is necessary to stabilize the high-temperature state, which is not yet achieved in the Cs-doped sample.

Conclusion

Using NMR spectroscopy and molecular modeling, subtle structural and major dynamical changes have been described for the hydrogen bonding of the intercalate water and surface silanol protons of the structure of the hydrous layer silicate Na−RUB-18 as functions of temperature. In the fortunate case of Na−RUB-18, this is possible because of the perfect crystalline order of the layer silicate. However, most of the structurally and chemically related hydrous layer silicates are disordered, statically and/or dynamically, thus hampering a detailed structural analysis. Therefore, the results presented here can be regarded as an example for other hydrous layer silicates. Using a combination of NMR experiments and modeling calculations, a deeper understanding of the physical properties of these materials can be achieved. These properties might change considerably at elevated temperatures, e.g., NA-RUB-18 becomes a 1D proton conductor, thus opening an interesting field of investigation.

CM0012522